The Impact of Comet Shoemaker-Levy 9 Sends Ripples Through the Rings of Jupiter

Mark R. Showalter, *et al.*

Science **332**, 711 (2011);
DOI: 10.1126/science.1202241

References and Notes

1. M. M. Hedman *et al.*, *Icarus* **188**, 89 (2007).
2. M. E. Ockert-Bell *et al.*, *Icarus* **138**, 188 (1999).
3. M. R. Showalter, M. M. Hedman, J. A. Burns, *Science* **332**, 711 (2011).
4. C. D. Murray, S. F. Dermott, *Solar System Dynamics* (Cambridge Univ. Press, Cambridge, 1999).
5. For Saturn's C ring, higher-order gravity harmonics, mainly J_4 (*6*), only contribute a total of <10% to the nodal regression rate and 10 to 15% to the gradient of the nodal regression rate.
6. R. A. Jacobson *et al.*, *Astron. J.* **132**, 2520 (2006).
7. H. A. Zebker, E. A. Marouf, G. L. Tyler, *Icarus* **64**, 531 (1985).
8. P. A. Rosen, G. L. Tyler, E. A. Marouf, J. J. Lissauer, *Icarus* **93**, 25 (1991).
9. The error estimate includes ±10 days of statistical error, ±13 days uncertainty from the published estimate of J_6 (*6*), ±13 days from allowing J_8 to range between 0 and −0.00001, and ±5 days that depends on whether the wavenumbers are corrected for the ring's predicted mass. Additional uncertainty could be introduced if J_{10} and higher-order terms in Saturn's gravity field are sufficiently large.
10. J. N. Cuzzi *et al.*, in *Saturn From Cassini-Huygens*, M. K. Dougherty, L. W. Esposito, S. M. Krimigis, Eds. (Springer, New York, 2009), pp. 459–509.
11. J. V. Scotti, H. J. Melosh, *Nature* **365**, 733 (1993).
12. E. Asphaug, W. Benz, *Icarus* **121**, 225 (1996).
13. M. Montalto, A. Riffeser, U. Hopp, S. Wilke, G. Carraro, *Astron. Astrophys.* **479**, L45 (2008).
14. Scenarios in which the debris from the disrupted comet hits the rings before it can leave the inner Saturn system are explored in SOM text 8 and are found to be less probable.
15. D. M. Kary, L. Dones, *Icarus* **121**, 207 (1996).
16. H. F. Levison, M. J. Duncan, *Icarus* **127**, 13 (1997).
17. K. Zahnle, P. Schenk, H. Levison, L. Dones, *Icarus* **163**, 263 (2003).
18. H. F. Levison, M. J. Duncan, K. Zahnle, M. Holman, L. Dones, *Icarus* **143**, 415 (2000).
19. S. Charnoz, A. Morbidelli, L. Dones, J. Salmon, *Icarus* **199**, 413 (2009).
20. This rate may be conservative because none of the referenced simulations include Saturn's rings, which could not only disrupt incoming comets but also withdraw some momentum from the debris, increasing its chances of being captured into orbit around Saturn.
21. A. Sánchez-Lavega *et al.*, *Astrophys. J.* **715**, L155 (2010).
22. C. C. Porco *et al.*, *Space Sci. Rev.* **115**, 363 (2004).

Acknowledgments: We acknowledge the support of the Imaging Science Subsystem team and the Cassini Project, as well as NASA's Planetary Geology and Geophysics, and Cassini Data Analysis programs. We also thank M. R. Showalter, P. D. Nicholson, S. Charnoz, L. Dones, and D. P. Hamilton for useful conversations.

Supporting Online Material

www.sciencemag.org/cgi/content/full/science.1202238/DC1
SOM Text
Figs. S1 to S5
Tables S1 to S3
References

27 December 2010; accepted 16 March 2011
Published online 31 March 2011;
10.1126/science.1202238

The Impact of Comet Shoemaker-Levy 9 Sends Ripples Through the Rings of Jupiter

Mark R. Showalter,[1]* Matthew M. Hedman,[2] Joseph A. Burns[2]

Jupiter's main ring shows vertical corrugations reminiscent of those recently detected in the rings of Saturn. The Galileo spacecraft imaged a pair of superimposed ripple patterns in 1996 and again in 2000. These patterns behave as two independent spirals, each winding up at a rate defined by Jupiter's gravity field. The dominant pattern originated between July and October 1994, when the entire ring was tilted by about 2 kilometers. We associate this with the Shoemaker-Levy 9 impacts of July 1994. New Horizons images still show this pattern 13 years later and suggest that subsequent events may also have tilted the ring. Impacts by comets or their dust streams are regular occurrences in planetary rings, altering them in ways that remain detectable decades later.

On 9 November 1996, the Galileo spacecraft imaged a systematic, unexplained pattern of brightness variations in Jupiter's main ring, suggesting vertical ripples in the ring's surface (*1*). More recently, Cassini images have revealed a similar pattern in Saturn's rings. The latter pattern arose from an initially inclined ring, which was slowly twisted into a spiral by Saturn's gravity (*2*, *3*). A closer analysis of Galileo data now confirms that the patterns in the rings of Jupiter and Saturn obey identical kinematics, except that Jupiter's ring contains two ripple patterns, not one.

Galileo viewed the rings from nearly edge-on, with opening angle $B = 0.48°$ (Fig. 1 and table S1). The intensity I of an optically thin ring is proportional to the amount of material along the line of sight, so it varies as $\sin(B)^{-1}$. For the jovian ring, optical depth $\tau < 10^{-5}$ (*4*, *5*), so this dependence applies. In this limit, the Sun's opening angle plays no role, because every particle is illuminated equally.

A nonzero surface slope modifies the effective local opening angle, naturally leading to variations in I (*6*).

$$I \propto 1/\sin(B)[1 - \sin(\theta)/\sin(B)Z'(R,\theta)] \quad (1)$$

Here, $Z(R,\theta)$ describes the local height of the ring above the equatorial plane in polar coordinates (R,θ). The radial component of the local slope is $Z'(R,\theta) \equiv \partial Z/\partial R$; we neglect the slope's much smaller tangential component (*6*, *7*). Longitudes are measured from the ansa line passing through the ring's tip, where a radial vector is perpendicular to the line of sight.

The dependence of I on $\sin(\theta)$ naturally predicts the reversals of contrast observed in the Galileo image. We have applied Eq. 1 to derive the function $Z'(R)$ at $\theta = 0$ (Fig. 1C). Slopes approach 3% or ~1.5°. However, unlike the pattern in Saturn's rings (*2*, *3*), this one is not a pure sinusoid; a Fourier transform shows two distinct peaks (Fig. 2A). In a least-squares modeling of $Z'(R)$, two sinusoids successfully account for the location of nearly every peak and trough. Matches to the amplitudes are imperfect, however, suggesting that the ring slope may be modulated by other factors that we have not yet considered. The dominant pattern has a wavelength $\lambda_{long} = 1920 \pm 150$ km and a vertical amplitude $Z_{long} = 2.4 \pm 0.7$ km; the shorter-wavelength pattern has $\lambda_{short} = 630 \pm 20$ km and $Z_{short} = 0.6 \pm 0.2$ km.

If these sinusoidally varying slopes are analogous to the corrugations observed at Saturn (*2*, *3*), then they arose from an initially tilted ring that slowly twisted into a spiral pattern as a result of differential nodal regression. The wavelength of these patterns depends only on the local gravitational field and the amount of time T that has elapsed since the ring became tilted (*2*, *3*). Near the middle of the main jovian ring, the predicted wavelength is

$$\lambda = \sim 4200 \text{ km}/(T/\text{years}) \quad (2)$$

The numerical factor is derived from Jupiter's gravitational harmonics (*8*). It varies by ~15% within the radial limits considered but for practical purposes can be treated as a constant when modeling individual profiles (*6*).

Compared with Saturn's ~30-km periodicity, the longer wavelengths at Jupiter would imply much more recent features. For the long-wavelength pattern, $T = 800 \pm 60$ days, indicating that a ring-tilting event occurred between 1 July and 1 November 1994. The shorter wavelength corresponds to $T = 2430 \pm 80$ days, meaning that the feature originated between early January and early June 1990; the midpoint is 19 March.

Two Galileo images from 21 June 2000 confirm that this pattern is evolving in the predicted

[1]SETI Institute, 189 Bernardo Avenue, Mountain View, CA 94043, USA. [2]Department of Astronomy, Cornell University, Ithaca NY 14853, USA.

*To whom correspondence should be addressed. E-mail: mshowalter@seti.org

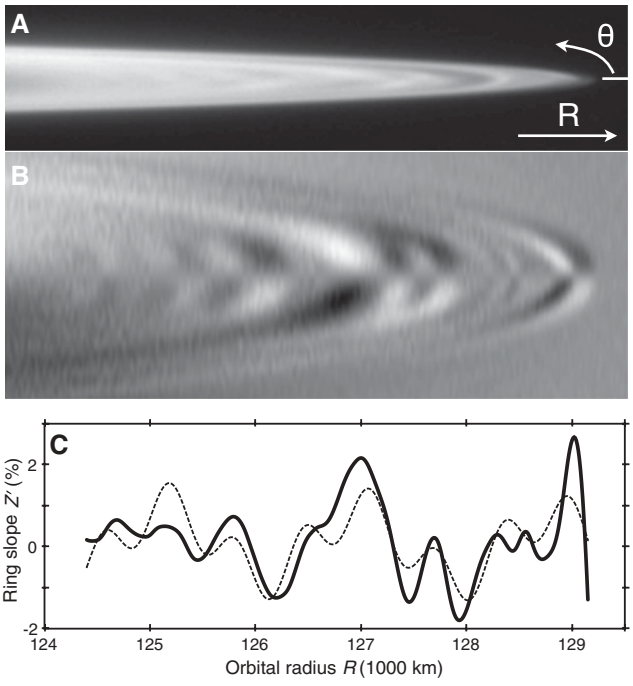

Fig. 1. (**A**) Galileo image C0368974139 from 9 November 1996 shows the jovian ring's tip. Indicated are the directions in which longitude θ and radius *R* are measured. (**B**) We expanded the image vertically, co-added two similar frames for improved signal-to-noise ratio, and subtracted a duplicate of the image after reversing it top-to-bottom. Most of the image nearly cancels itself out, but the signals of the ripples are reinforced. Neutral gray corresponds to zero; darker areas are negative. (**C**) A derived profile of the ring's surface slope versus radius (solid line). For comparison, the dashed line shows a fit involving superimposed patterns triggered on 19 July 19 and 19 March 1990. In this fit, we have neglected the expected variation in λ with *R* (*6*). Panels (A) to (C) have been aligned vertically to employ the same radial/horizontal scale.

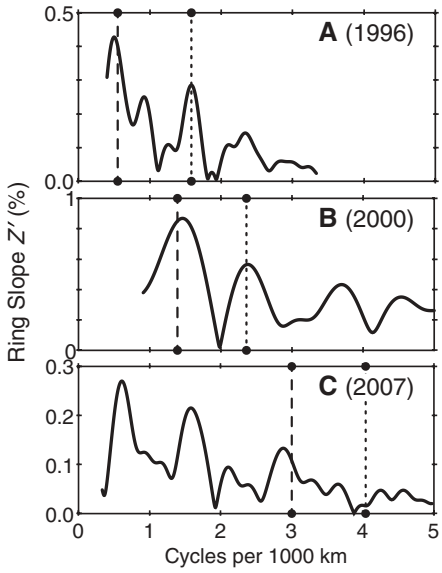

Fig. 2. Fourier transforms of each radial profile of the ring's surface slope, $Z'(R)$. Data are from Galileo in 1996 (**A**) and 2000 (**B**) and from New Horizons in 2007 (**C**). Vertical lines mark the expected wave number (1/λ) for features triggered on 19 July 1994 (dashed) and on 19 March 1990 (dotted). On the vertical axes, the Fourier amplitude values roughly indicate the height of a single sinusoid, of fixed wavelength but variable phase, that best fits the profile.

manner. The images individually have very poor signal-to-noise properties, and charged particle impacts into the camera's charge-coupled device corrupt many pixels (fig. S1). Nevertheless, combined processing of both images has enabled us to identify and eliminate most of the corrupted pixels (Fig. 3A). Contrast reversals show up clearly after processing (Fig. 3B), from which we have derived $Z'(R)$ (Fig. 3C). Fourier processing once more identifies two dominant peaks, but now they are at shorter wavelengths (Fig. 2B). Modeling of the ring profile as a superposition of two sinusoids provides a very good description of the data (Fig. 3C, dashed line), with $\lambda_{long} = 695 \pm 55$ km; $Z_{long} = 1.8 \pm 0.4$ km; $\lambda_{short} = 414 \pm 20$ km; $Z_{short} = 0.6 \pm 0.2$ km. For comparison, if we use Eq. 2 to extrapolate forward the patterns seen in 1996 over the intervening 1289 days, we would expect $\lambda_{long} = 734$ km and $\lambda_{short} = 412$ km. Thus, the wavelengths and amplitudes seen in 2000 are consistent with the expected rate of winding of these spiral features.

To complete our data analysis, we examined four images taken just before New Horizons crossed the jovian ring plane on 1 March 2007 (figs. S2 to S4). Fourier analysis reveals the lingering effects of the 1994 ring-tilting event (Fig. 2C). Although λ_{long} has diminished to ~350 km, this detection attests to the features' longevity. The shorter pattern can no longer be detected. However, two suggestive new patterns appear, with $\lambda \approx 1315$ km and 775 km (fig. S4C). If confirmed by later detections, these would indicate that the rings received additional km-scale tilts around September 2001 and December 2003.

A suitable explanation for ring-tilting events must satisfy some very specific requirements. First, each event must occur within a very brief time span (*2*, *3*). The nodal regression rate for orbits in the main jovian ring is 8.5°/day, enough to smear out the effects of any event lasting more than a few weeks. Second, these events must be infrequent, with 2 to 4 occurrences between ~1985 and ~2006. Within this context, it is natural to associate the long pattern with the Shoemaker-Levy 9 (SL9) impacts of 16 to 20 July 1994. They occurred within the identified window spanning July to October. Although SL9 was earlier regarded as a "once a century" impact, the observed collision of another object into Jupiter on 19 July 2009 suggests that such events may be 5 to 10 times more frequent than previously thought (*9*). The chance of one occurring at random within the identified 4-month window is 1 to 3%.

The triggering event for the secondary pattern in Galileo images is less clear. SL9 fractured during its previous perijove on 7 July 1992. It crossed the equator at $R \sim 115{,}000$ km (*10*), apparently producing no measurable effect on the ring less than 15,000 km further out. The perijove before that was in mid-1990, within the window defined by the short wavelength and raising the possibility that SL9 triggered this pattern as well. However, backward integrations of SL9's trajectory place this perijove much farther from Jupiter (*10*, *11*). Such integrations have large uncertainties, arising from the chaotic nature of SL9's orbit, and because we do not know where to position the center of SL9's mass before its breakup (*10*, *11*). Thus, we cannot rule out the possibility that SL9 triggered the 1990 pattern, although it must have passed much closer to the ring than it did in 1992. Alternatively, the secondary pattern may have been triggered by a different, unseen comet; this hypothesis is generally compatible with more recent, higher estimates of the frequency of impacts (*9*). History records other very close passages of Jupiter by comets 16P/Brooks 2 in 1886 and P/Gehrels 3 in 1970 (*12*).

What mechanism might have enabled SL9 to alter the jovian ring so dramatically? In 1994, SL9's solid fragments entered Jupiter at southern latitudes on a north-bound trajectory; they never reached the ring plane. However, dust grains associated with SL9's fragments could have been deflected past the planet and into the ring by solar radiation pressure (Fig. 4) (*6*). Others have explored the effects of radiation pressure on SL9's dust (*13*, *14*), but not with an eye toward the consequences for the ring system. We define β as the ratio of radiation pressure to solar gravity (*15*). Integrations show that grains with $\beta = 0.007$ (radius ≈ 50 μm), if released at the time of the 1992 perijove and breakup, would be deflected directly into the main ring in 1994 (*6*). Larger grains can never intercept the ring, but smaller ones, if released later, can. The fragments were emitting dust continuously between the 1992 breakup and the 1994 impact (*14*, *16*), providing a continuous source of potential ring impactors. Regardless of their ejection date, integrations show that all particles crossing the main jovian ring do so within the same ~10° sector of inertial longitude and within a time span of a few days (*6*); thus, they naturally satisfy the requirement to offset the ring quickly and systematically.

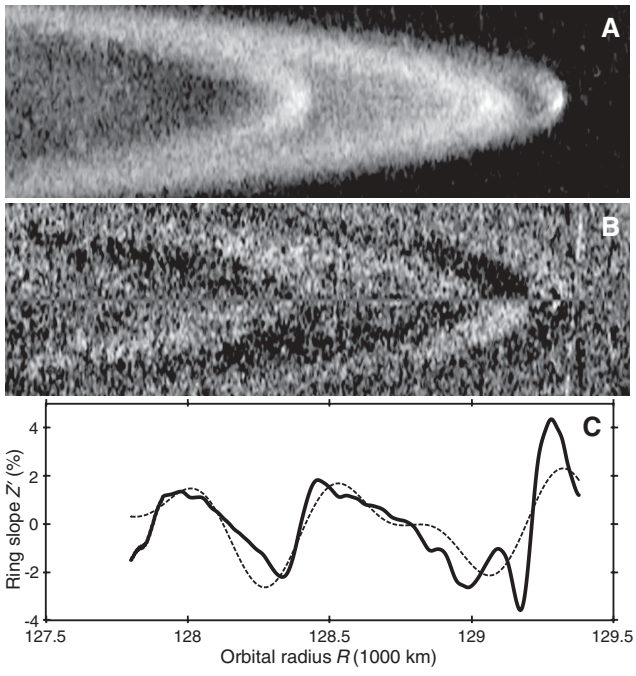

Fig. 3. (**A**) Two Galileo images from 2000 have been overlaid and combined to produce a clear image of the ring's ansa (*6*). (**B**) After flipping the image vertically and subtracting, enhancement reveals the pattern of contrast reversals indicating vertical undulations. (**C**) A derived radial profile of the ring's slope (solid line). For comparison, the dashed line is a best fit using two sinusoidal patterns, with wavelengths defined by our assumed trigger dates of 19 July 1994 and 19 March 1990. The three panels have been aligned to employ the same radial scale; note that this scale is much smaller than that in Fig. 1.

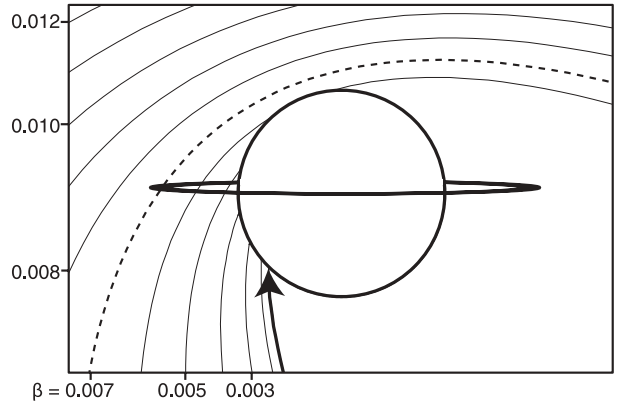

Fig. 4. The influence of solar radiation pressure on the motion of SL9's fragments is shown as a function of β. Integrations assume that the pieces separated at low relative velocity during the 1992 perijove. The heavy arrow (β = 0) shows the path of the large, observed fragments. The trajectories of smaller particles are displaced leftward in the diagram; corresponding β values are labeled around the periphery. Particles with β ≈ 0.007 (heavy dashed line) impact the main ring.

Because Jupiter's ring is optically thin, every ring constituent responds independently to the influx of cometary dust. To tilt an orbit by 2 km requires that, on average, particles intercept ~10^{-6} their own mass (*6*). For a ring of 1-cm particles spanning the orbits of Metis and Adrastea (128,000 to 129,000 km), an integrated fluence of ~10^{-6} g/cm^2 would be required, or ~10^{13} g in total. Our simulations indicate that 0.2 to 0.5% of SL9's ejecta smaller than 50 μm will intercept this ring (*6*). We therefore require SL9 to produce ~2 × 10^{15} to 5 × 10^{15} g of dust, amounting to a volume ~2 to 5 km^3. For comparison, estimates of the initial diameter of the intact comet range from D ~ 1.5 km (*17*) to 10 km (*18*). Corresponding volume estimates are V = 2 to 500 km^3. A meta-study (*19*) concludes D = 3.5 km (V ≈ 20 km^3). The fragments of SL9 underwent substantial collisional evolution shortly after the breakup (*13*); this can lead to a steep size distribution in which a substantial fraction of the mass is concentrated in the smallest particles. If so, then the larger estimates for SL9's volume are compatible with our requirements. Our results are difficult to reconcile with the smallest size estimates, which are based on dynamical models of how a loosely bound rubble pile would break apart (*17*).

For a given fluence of cometary dust, larger ring bodies are deflected to smaller tilt angles in inverse proportion to their radii. We chose 1 cm for the above calculation because cm-sized particles are likely to achieve the largest tilts; smaller particles can be shattered by the 50-μm impactors (*6*). Thus, our mass estimate is only valid if the size distribution is steep, so that the ring's appearance is dominated by the smallest surviving particles (and their ejecta). The jovian ring's dust population does steepen markedly above ~30 μm (*5*), suggesting that this assumption is plausible.

The kinematics of these spirals requires that the wavelength be nearly uniform at any given time, but the tilts need not be. In an optically thin ring, they will vary depending on the local ring particle sizes. In Fig. 1C, the inward decrease of the slopes may simply indicate a decreasing population of the cm-sized particles. This is consistent with ring photometry that indicates a rapidly decreasing number of embedded macroscopic bodies interior to the orbit of Metis (*20*, *21*).

We now recognize that impacts by comets and/or their dust clouds are common occurrences in planetary rings. On at least three occasions over the past few decades, these collisions have carried sufficient momentum to tilt a ring of Jupiter or Saturn off its axis by an observable distance. Once such a tilt is established, it can persist for decades, with the passage of time recorded in its ever-tightening spiral. Within these subtle patterns, planetary rings chronicle their own battered histories.

References and Notes

1. M. Ockert-Bell *et al.*, *Icarus* **138**, 188 (1999).
2. M. M. Hedman *et al.*, *Icarus* **188**, 89 (2007).
3. M. M. Hedman, J. A. Burns, M. W. Evans, M. S. Tiscareno, C. C. Porco, *Science* **332**, 708 (2011).
4. M. R. Showalter, J. A. Burns, J. N. Cuzzi, J. B. Pollack, *Icarus* **69**, 458 (1987).
5. S. M. Brooks, L. W. Esposito, M. R. Showalter, H. B. Throop, *Icarus* **170**, 35 (2004).
6. Materials and methods are available as supporting material on *Science* Online.
7. This formula is only valid where both sin(*B*) and sin(θ)/sin(*B*) $Z'(R,\theta)$ are << 1; these constraints are satisfied throughout our analysis.
8. R. A. Jacobson, *Bull. Am. Astron. Soc.* **33**, 1039 (2001).
9. A. Sánchez-Lavega *et al.*, *Astrophys. J.* **715**, L155 (2010).
10. L. A. Benner, W. B. McKinnon, *Icarus* **118**, 155 (1995).
11. P. W. Chodas, D. K. Yeomans, in *The Collision of Comet Shoemaker-Levy 9 and Jupiter*, K. S. Noll, H. A. Weaver, P. D. Feldman, Eds. (Cambridge Univ. Press, Cambridge, 1996), pp. 1–30.
12. K. Zahnle, L. Dones, H. F. Levison, *Icarus* **136**, 202 (1998).
13. Z. Sekanina, P. W. Chodas, D. W. Yeomans, *Astrophys. J.* **289**, 607 (1994).
14. J. M. Hahn, T. W. Rettig, *Icarus* **146**, 501 (2000).
15. J. A. Burns, P. L. Lamy, S. Soter, *Icarus* **40**, 1 (1979).
16. H. A. Weaver *et al.*, *Science* **263**, 787 (1994).
17. E. Asphaug, W. Benz, *Icarus* **121**, 225 (1996).
18. Z. Sekanina, P. W. Chodas, D. K. Yeomans, *Planet. Space Sci.* **46**, 21 (1998).
19. M. Zamarashkina, Y. Medvedev, *Proc. ACM* **500**, 457 (2002).
20. J. A. Burns *et al.*, in *Jupiter: The Planet, Satellites and Magnetosphere*, F. Bagenal, Ed. (Cambridge Univ. Press, Cambridge, 2004), pp. 241–262.
21. M. R. Showalter *et al.*, *Science* **318**, 232 (2007).

Acknowledgments: M.R.S. acknowledges the support of NASA's Jupiter Data Analysis Program through grant NNX09AD97G. J.A.B. has been funded by NASA's Planetary Geology and Geophysics Program.

Supporting Online Material

www.sciencemag.org/cgi/content/full/science.1202241/DC1
Materials and Methods
Figs. S1 to S5
Table S1
References 22 and 23

27 December 2010; accepted 16 March 2011
Published online 31 March 2011;
10.1126/science.1202241